High-energy astrophysical neutrinos from cosmic strings

Cyril Creque-Sarbinowski,[1,*] Jeffrey Hyde,[2,3] and Marc Kamionkowski[1]
[1]*William H. Miller III Department of Physics and Astronomy, Johns Hopkins University, 3400 North Charles Street, Baltimore, Maryland 21218, USA*
[2]*Department of Physics and Astronomy, Bowdoin College, 8800 College Station, Brunswick, Maine 04011-8488, USA*
[3]*Department of Physics, Moravian University, 1200 Main Street, Bethlehem, Pennsylvania 18018, USA*

(Received 13 June 2022; accepted 2 May 2023; published 15 June 2023)

Cosmic strings that couple to neutrinos may account for a portion of the high-energy astrophysical neutrino (HEAN) flux seen by IceCube. Here, we calculate the observed spectrum of neutrinos emitted from a population of cosmic-string loops that contain quasicusps, quasikinks, or kink-kink collisions. We consider two broad neutrino emission models: one where these string features emit a neutrino directly, and one where they emit a scalar particle which then eventually decays to a neutrino. In either case, we find the spectrum of cosmic-string neutrinos to follow a two-parameter model described by a power law with a high-energy cutoff. While none of the models in question fully match the observed HEAN spectrum, we do find that the maximum contribution of cosmic-string neutrinos can still be an $\mathcal{O}(1)$ fraction of the observed flux in addition to producing a bump in the observed neutrino spectrum. Finally, for each of the models presented, we present the viable parameter space for neutrino emission.

DOI: 10.1103/PhysRevD.107.123019

I. INTRODUCTION

IceCube routinely detects high-energy astrophysical neutrinos (HEANs) with TeV-PeV energies that follow a power law flux spectrum with spectral index $\gamma \sim 2.28$ [1,2]. Explanations for the source of this flux have ranged from gamma-ray bursts [3–9], to Fanaroff–Riley type 0 (FR0) quasars [10], blazars [11–13], radio-bright active galactic nuclei [14–16], choked jet supernovae [17,18], pulsar wind nebulae [19], and more. However, none of these propositions have been confirmed as the dominant source of the observed spectrum [20]. One additional possibility is that cosmic-string loops source these neutrinos. More concretely, the actual mechanism of emission could be due to the radiation of particles from string features, known as quasicusps, quasikinks, or kink-kink collisions, that generically occur during the evolution of cosmic-string loops. These particles could either be the neutrinos themselves (direct neutrino emission) or a parent particle which then decays into neutrinos (indirect neutrino emission).

The emission of neutrinos due to the decay of a real scalar radiated from cusps and kinks has previously been considered in the ultrahigh energy range [21,22]. Moreover, the energy spectrum of various Standard Model (SM) particles near the string has been extensively computed in the context of dark strings coupling through the Higgs portal operator [23–25]. More generally, the program of calculating emission from cosmic strings also includes the radiation of gravitational waves, cosmic rays, and more [26–31].

In this work we extend and refine these calculations in several manners. First, we calculate the optical depth of HEANs using all seven channels of Standard Model neutrino self-interactions and thus including the energy dependence of the neutrino horizon. Then, we perform this calculation for all three types of string features: quasicusps, quasikinks, and kink-kink collisions. Prior work has only considered the first two in the scenario of neutrino emission. In addition, we calculate the emission from a real scalar not only in the scenario of a cascade (casc) of particles, but also the direct decay into neutrinos. Moreover, we present the first calculation for the emission of neutrinos directly from cosmic strings via a two-body decay interaction and the Aharonov-Bohm coupling. Finally, we incorporate the shrinking of loops due to particle radiation into the loop distribution function, a factor ignored in earlier neutrino emission papers. Using these calculations, we present the viable parameter space for neutrino emission for each of the models chosen. Moreover, we find that for these models, cosmic strings can still contribute an $\mathcal{O}(1)$ fraction of the observed HEAN flux. Since the models represent a wide selection of possible emission mechanisms, we conclude it is unlikely

*creque@jhu.edu

that a single population of cosmic strings can create the entirety of the HEAN background. However, as a subdominant component, cosmic strings may still contribute enough to create a bump in the spectrum.

This paper is organized as follows. In Sec. II we present the general formalism in order to calculate the differential flux of neutrinos observed at IceCube from an arbitrary source and then particularize to the case of a cosmic-string loop population. For this population, we introduce four interaction terms between cosmic strings and neutrinos using an effective field theory approach in Sec. III. These interactions cover both direct and indirect neutrino emission, each of which is split into two further cases. We use these interaction terms to then calculate the energy spectrum of neutrinos emitted at the locality of the string in Sec. IV. We follow up this calculation and then specify the form of the cosmic-string loop number density in Sec. V. Ultimately, we combine both the energy spectrum of neutrinos with the cosmic-string loop number density to calculate the observed differential flux of neutrinos through the formalism presented in the beginning, shown in Eq. (37). Using this flux, we constrain both the fraction of neutrinos attributed to emission from cosmic strings in the IceCube spectrum and the phenomenological parameter space for neutrino emission in Sec. VI. We discuss and conclude in Secs. VII and VIII.

II. NEUTRINO SPECIFIC FLUX

The specific flux $\Phi_i(t,E)$ of neutrinos ν_i (number of astrophysical neutrinos per unit conformal time per unit comoving area per unit energy) at cosmic time t and observed energy E from a source S_i is [32]

$$\Phi_i(t,E)=\int_{-\infty}^{t} dt'[a(t)/a(t')]e^{-\tau_i(t',t,E)}S_i\{t',[a(t)/a(t')]E\}, \tag{1}$$

where $a(t)$ is the scale factor and $\tau_i(t',t,E)$ is the optical depth of a neutrino ν_i of energy E between times t' and t.

For a single cosmic-string loop, the spectrum of emitted neutrinos is a function of the loop length L, and so the source function is the integral over all loop contributions,

$$S^e_{i,a}(t,E)=\sum_a c\int_0^\infty dL\,\frac{d\dot{N}^e_{i,a}(t,L,E)}{dN_{\rm loop}dE}\frac{dn_{\rm loop}(t,L)}{dL}, \tag{2}$$

with $dn_{\rm loop}(t,L)/dL$ the number of cosmic-string loops per comoving volume per loop length, and $d\dot{N}^e_{i,a}/dN_{\rm loop}dE$ the number of neutrinos ultimately produced from string feature a and emission model e per unit time per loop per neutrino energy E. The string features we consider are quasicusps, quasikinks, and kink-kink collisions, shown in Fig. 1, so that the label a takes values $a\in\{qc,qk,kk\}$. We present the different emission models in Sec. III. In general,

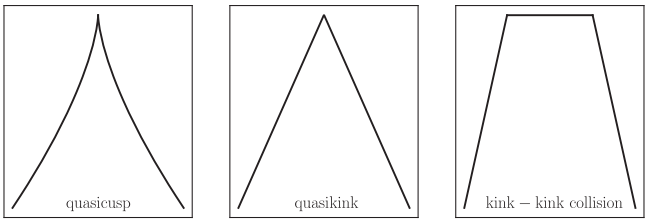

FIG. 1. Picture of quasicusps, quasikinks, and kink-kink collisions.

a loop can contain multiple features at once (e.g., a string could have four kinks and a quasicusp). Here, for simplicity, we assume that only a single feature exists on every loop. However, we note that, for a given type of feature, multiple features can be incorporated straightforwardly by linearly scaling the amplitude of emission by the corresponding number. We then write the emitted neutrino spectrum as

$$\frac{d\dot{N}^e_{i,a}(t,L,E)}{dN_{\rm loop}dE}=\frac{1}{[(L/2)/c]}\int dE_p\,\frac{dN^e_i(E,E_p)}{dN^e_a dE}\frac{dN^e_a(E_p,L)}{dE_p}, \tag{3}$$

with $[(L/2)/c]$ the period of oscillation for a cosmic-string loop, $dN^e_i/dN^e_a dE$ the number of neutrinos emitted per parent particle per unit neutrino energy E, and dN^e_a/dE_p the number of parent particles emitted from string feature a per unit parent particle energy E_p.

If neutrinos are emitted directly from the cosmic string and there is no parent particle, we set $dN^e_i(E,E_p)/dN^e_a dE(E,E_p)=\delta(E-E_p)\delta^i_e$ with $\delta(x)$ the Dirac delta function and δ^j_i the kronecker delta function that determines if the neutrino i is the same as the emitted particle in emission model e.

Roughly speaking, the cosmic-string phenomenology is then encoded in the emitted neutrino spectrum, and the cosmic-string population dynamics in its number density.

Neutrino self-interactions (νSI) in the SM induce scattering between HEANs and cosmic background neutrinos and thus a nonzero HEAN optical depth. We evaluate the total HEAN optical depth following Ref. [33], including all seven channels of SM νSI. These channels lead to a sharply defined neutrino horizon at redshift z_{ν_i}. That is, an observer located at redshift $z(t)$ will not see neutrinos of a given energy E originating from a redshift $z(t')>z_{\nu,i}(t,E)$. Therefore, in order to simplify our expressions, we will take the following approximation,

$$D_{\nu_i}(t',t,E)\equiv e^{-\tau_i(t',t,E)}=\Theta[z_{\nu_i}(t,E)-z(t')], \tag{4}$$

for the damping factor, with z_{ν_i} defined by the expression $D_{\nu_i}\{t'[z_{\nu,i}(t,E)],t,E\}=\exp(-1)$. We show both the

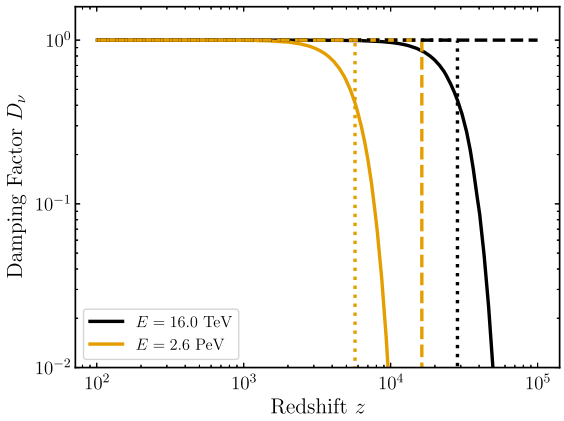

FIG. 2. The HEAN damping factor D_{ν_i}. The solid lines indicate the complete damping factor, the dashed the approximation given by Ref. [21], and the dotted are given by our approximation in Eq. (4).

complete HEAN optical depth and our approximation in Fig. 2 for some typical energies.

III. COSMIC-STRING PHENOMENOLOGY

Cosmic strings are topological defects formed after a $U(1)$ symmetry-breaking phase transition occurs in the Universe and are characterized by their tension μ. Then there are two broad phenomenological categories by which neutrinos may be emitted from this string. First, the string may directly couple to neutrinos. Second, it may indirectly couple to neutrinos; i.e., it may emit some intermediary particle which then eventually converts to some number of neutrinos. In either case, we model the free string loop action using the Nambu-Goto action for an infinitely long straight string, as locally the string loop is straight, regardless of any features

$$\mathcal{L}_{\rm str} = -\frac{\mu}{\hbar c}\int d^2\sigma\sqrt{-\gamma}\delta^4[x^\mu - X^\mu(\sigma,\tau)], \tag{5}$$

where $\hbar$ is Planck's constant, $g \equiv \det g_{\mu\nu}$ is the determinant of the spacetime metric $g_{\mu\nu}$, and γ the analogous quantity for the induced worldsheet metric $\gamma_{ab} = g_{\mu\nu}X^\mu_{,a}X^\nu_{,b}$ with worldsheet coordinates (σ,τ). We take the background metric to be flat $g_{\mu\nu} = \eta_{\mu\nu} = \mathrm{diag}(-1,1,1,1)$.

This string has a stress-energy tensor

$$T^{\rm str}_{\mu\nu}(x^\mu) = \frac{-\mu}{\sqrt{-g}}\int d^2\sigma\sqrt{-\gamma}\gamma_{ab}X^a_\mu X^b_\nu\delta^4[x^\mu - X^\mu(\sigma,\tau)] \tag{6}$$

with trace

$$T_{\rm str}(x^\mu) = -2\mu\int d^2\sigma\sqrt{-\gamma}\delta^4[x^\mu - X^\mu(\sigma,\tau)], \tag{7}$$

where we neglect any backreaction of interactions onto the string as for the models we consider they are small. When considering interactions with this string we take an effective field theory approach and remain agnostic to any particular ultraviolet theory constraints. We note that, strictly speaking, the string tension is a function of such interactions. However, in practice, the dependence is very weak [23], and hence the tension can be considered an independent parameter from the couplings we discuss in the following.

A. Direct coupling

For simplicity, we consider only a single neutrino species of mass $m_\nu = \hbar/(c\lambda_\nu)$ and take it to be a Dirac fermion. Thus its free Lagrangian is

$$\mathcal{L}^\nu_{\rm free} = -\bar\nu(i\gamma^\mu\partial_\mu - \lambda_\nu^{-1})\nu, \tag{8}$$

with γ^μ the gamma matrices. There are two versions of direct cosmic-string coupling we consider. First, the neutrinos may couple directly to the string worldsheet through a two-body interaction, so that its interaction is

$$\mathcal{L}^{(2)}_{\rm int} = \frac{g^{(2)}}{2}\left(\frac{\hbar c}{\mu^3}\right)^{1/2}\bar\nu\nu T_{\rm str}, \tag{9}$$

with $g^{(2)}$ the two-body interaction coupling. Second, neutrinos may couple through some gauge flux that permeates through the string in an Aharonov-Bohm (AB) fashion [34]

$$\mathcal{L}^{\rm AB}_{\rm int} = g_\nu\bar\nu\gamma^\mu V_\mu\nu, \tag{10}$$

with g_ν the charge of the neutrino under V_μ, V_μ a classical background field induced by the flux $\Phi = (2\pi/g_\nu)\theta_q$ the string carries, and θ_q the AB phase around the string. In the Lorentz gauge, this background field is written as [35]

$$V_\mu = -\frac{i\Phi}{2}\int\frac{d^4k}{(2\pi)^4}\frac{p^\nu}{p^2}\int d\sigma_{\mu\nu}e^{-ik\cdot[x^\mu - X^\mu(\sigma,\tau)]}, \tag{11}$$

with $d\sigma_{\mu\nu} = d^2\sigma\epsilon^{\mu\nu\alpha\beta}\epsilon^{ab}X^\alpha_{,a}X^\beta_{,b}$ the worldsheet area element and $\epsilon^{i..j}$ the Levi-Civita symbol. Note that this field has support outside of the string, unlike the purely local interaction considered above.

B. Indirect coupling

For indirect emission of neutrinos, we consider the intermediary particle to be a real scalar ϕ of mass $m_\phi = \hbar/(c\lambda_\phi)$. As a result, there is only one cosmic-string Lagrangian to write down:

$$\mathcal{L} = \mathcal{L}_{\rm str} + \mathcal{L}^\phi_{\rm free} + \mathcal{L}^\phi_{\rm int}, \tag{12}$$

$$\mathcal{L}^{\phi}_{\rm free} = -\left(\frac{1}{2}\partial_\mu\phi\partial^\mu\phi + \frac{1}{2}\lambda_\phi^{-2}\phi^2\right), \tag{13}$$

$$\mathcal{L}^{\phi}_{\rm int} = \frac{\alpha}{(4\mu\hbar c)^{1/2}}\phi T_{\rm str}, \tag{14}$$

with α as the scalar coupling constant.

In order to obtain neutrinos indirectly we consider two scenarios. First, the scalar particle decays directly into neutrinos via a Yukawa (Yu) interaction,

$$\mathcal{L}_{\rm Yu} = g_{\rm Yu}\bar{\nu}\phi\nu. \tag{15}$$

Alternatively, the scalar particle couples to some gauge boson—either a hidden sector gauge boson or the gluon, and these gauge fields have interactions which lead to a cascade of particles being emitted which end in neutrinos. For example, if it is the gluon, hadronic cascades produce pions which then lead to neutrino emission. For concreteness, we write down an example Lagrangian as

$$\mathcal{L}_{\rm casc} = \alpha\ell_{\rm P}\phi G_{\mu\nu}G^{\mu\nu}, \tag{16}$$

with $\ell_{\rm p}$ the Planck length and $G_{\mu\nu}$ the gluon field strength tensor.

IV. PARTICLE EMISSION

Given a model for cosmic-string interactions with neutrinos, we now write the number spectrum of particles emitted from cosmic-string loops. However, this spectrum depends not only on the phenomenology of the interactions, but also the feature of the string that emits the particle. Thus, in what follows, for each interaction considered we specify the type of feature as well.

In order to calculate the spectrum of emitted particles we take the leading-order S-matrix approach. Thus, we calculate the probability of creating a state $\langle k_1, s_1; \ldots; k_N, s_N|$ with N particles with momenta k_i and spin s_i out of the vacuum $|0\rangle$ given an interacting term,

$$\mathcal{A}_e(\mathbf{k},\mathbf{s}) = i\int d^4x\langle k_1, s_1; \ldots; k_N, s_N|\mathcal{L}^e_{\rm int}|0\rangle \tag{17}$$

$$dN^e_a = \sum_{i=1}^{N_s}\sum_{s_{a_i}}\prod_{j=1}^{N}\frac{d^3k_j}{(2\pi)^2\omega_j}|\mathcal{A}_e(\mathbf{k},\mathbf{s})|^2, \tag{18}$$

with N_s the number of particles with nonzero spins, N the number of particles, a_i the map from spin particle number to particle number (e.g., a particle could be the first particle with spin but the fifth overall particle in a list), and the sum s_{a_i} goes over the possible spin values of particle a_i. Lower bounds on the energy of the resulting spectrum arise from integrating over the worldsheet. Upper bounds on the energy of the spectrum arise from the requirement that the energy of the particle be smaller than the string energy scale. For more details we refer the reader to Ref. [24]. While both of these cutoffs in reality have a slight softening, they still decay rapidly, and so here we approximate them as sharp discontinuous transitions.

The average power emitted from a cosmic string over one period of oscillation is therefore

$$dP^e_a = \frac{1}{[(L/2)/c]}\sum_{i=1}^{N_s}\sum_{s_{a_i}}\prod_{j=1}^{N}\frac{d^3k_j}{(2\pi)^2\omega_j}\left(\sum_{k=1}^{N}\omega_k\right)|\mathcal{A}_e(\mathbf{k},\mathbf{s})|^2. \tag{19}$$

In order to complete the description of the string feature, several quantities must also be defined detailing the shape of the string feature in question. Rather than defining these quantities precisely, here we simply tabulate the numerical constants that encode their behavior, assuming that shape effects are $\mathcal{O}(1)$. Following this procedure, these constants then take a range of values: $\Theta \in [0.42, 3.6]$ and $\psi \in [0.047, 0.23]$. We define the rest of these constants in Table I. For a first-principle definition of these parameters and their values we refer the reader to Ref. [24].

A. Direct coupling

First, we present the spectrum of neutrinos directly emitted from cosmic string loops with quasicusps, quasikinks, and kink-kink collisions.

1. Two-body

For both quasicusps and quasikinks, the momenta of both emitted (nearly massless) fermions are parallel to one another, and thus the emission is helicity suppressed. For kink-kink collisions that emit relativistic neutrinos,

$$\frac{dN^{(2)}_{kk}}{dE} = \tilde{\Gamma}^{(2)}_{kk}\frac{E}{\mu\hbar c}\left[1+\left(\frac{E^2}{\mu\hbar c}\right)^{1/2}\right]^{-3}, \tag{20}$$

$$P^{(2)}_{kk} = \Gamma^{(2)}_{kk}\frac{\mu c}{L/\ell_{(2)}}, \tag{21}$$

with $m_\nu c^2 \ll E \leq (\mu\hbar c)^{1/2}$ and $\tilde{\Gamma}^{(2)}_{kk} = 4[g^{(2)}]^2\mathcal{S}_{kk}/(3\pi^2)$, $\Gamma^{(2)}_{kk} = (37/5)\tilde{\Gamma}^{(2)}_{kk}$ and $\ell_{(2)} = (\hbar c/\mu)^{1/2}$.

TABLE I. Range of values for cosmic-string shape-dependent amplitude, assuming the shape parameters are $\mathcal{O}(1)$.

a	Quasicusp	Quasikink	Kink-kink
$\mathcal{S}_a$	[0.2, 10]	[0.1, 20]	[1, 500]
$\mathcal{T}_a$	[0.5, 50]	[1, 200]	[0.2, 200]

2. Aharonov-Bohm

In AB emission, there are no obvious suppressions, and so we write down the spectrum and power for all emission types in the relativistic limit

$$\frac{dN_a^{\rm AB}}{dE} = \tilde{\Gamma}_a^{\rm AB}\left(\frac{\hbar c}{L}\right)^{q_a^{\rm AB}} \times\left[\frac{1}{(E+E_{\rm min}^{{\rm AB},a})^{1+q_a^{\rm AB}}}-\frac{1}{(E+E_{\rm max}^{{\rm AB},a})^{1+q_a^{\rm AB}}}\right], \quad (22)$$

$$P_a^{\rm AB} = \Gamma_a^{\rm AB}\frac{\mu c}{(L/\ell_{\rm AB})^{p_a^{\rm AB}}}, \quad (23)$$

with $\tilde{\Gamma}_{qc}^{\rm AB} = (2\pi\theta_q)^2\psi^{-4/3}\Theta^2/[32(2\pi)^4]\mathcal{T}_{qc}$, $\tilde{\Gamma}_{qk}^{\rm AB} = [3\mathcal{T}_{qk}/(4\mathcal{T}_{qc})](2/\Theta)\tilde{\Gamma}_{qc}^{\rm AB}$, $\tilde{\Gamma}_{kk}^{\rm AB} = (\mathcal{T}_{kk}/\mathcal{T}_{qc})(2\Theta^2)^{-1}\psi^{4/3}\tilde{\Gamma}_{qc}^{\rm AB}$, and $\ell_{\rm AB} = (\hbar c/\mu)^{1/2}$. We define all other variables in Table II.

B. Indirect coupling

Now, we present the spectrum of neutrinos indirectly emitted from cosmic string loops. More concretely, we first present the spectrum of real scalar particles directly emitted from string loops with quasicusps, quasikinks, and kink-kink collisions. Then, we write the spectrum of neutrinos emitted from a real scalar.

Once again, there are no obvious suppressions, and so the string feature spectra and emitted power are

$$\frac{dN_a^\phi}{dE_\phi} = \tilde{\Gamma}_a^\phi\left(\frac{E_\phi L}{\hbar c}\right)^{q_a^\phi}\frac{\mu\hbar c}{E_\phi^3}, \quad (24)$$

$$P_a^\phi = \frac{\Gamma_a^\phi \mu c}{(L/\ell_\phi)^{p_a^\phi}}, \quad (25)$$

with E_ϕ the lab frame energy of the ϕ particle (different from the neutrino energy E) and $\ell_\phi = \ell_{\rm Yu} = \ell_{\rm casc} = \lambda_\phi$. All other variable definitions are placed in Table III. After the real scalar is emitted, we assume it emits neutrinos instantaneously.

1. Yukawa

Through a Yukawa coupling, two neutrinos are emitted from the heavy real scalar ϕ with an isotropic (i.e., flat energy) spectrum

TABLE II. AB variable definitions.

a	Quasicusp	Quasikink	Kink-kink
$q_a^{\rm AB}$	0	1/3	0
$p_a^{\rm AB}$	1/2	4/3	1
$\Gamma_a^{\rm AB}$	$\log(16)\tilde{\Gamma}_{qc}^{\rm AB}$	$18(1-2^{-1/3})\tilde{\Gamma}_{qk}^{\rm AB}$	$\log(16)\tilde{\Gamma}_{kk}^{\rm AB}$
$E_{\rm min}^{{\rm AB},a}$	$\psi m_\nu c^2\sqrt{m_\nu cL/\hbar}$	$\psi m_\nu c^2\sqrt{m_\nu cL/\hbar}$	$m_\nu c^2$
$E_{\rm max}^{{\rm AB},a}$	$[(\mu^2L^2)(\mu\hbar c)]^{1/4}$	$(\mu\hbar c)^{1/2}$	$(\mu\hbar c)^{1/2}$

TABLE III. Variable definitions for the real scalar ϕ.

a	Quasicusp	Quasikink	Kink-kink
q_a^ϕ	2/3	1/3	0
p_a^ϕ	1/2	1	1
$\tilde{\Gamma}_a^\phi$	$\alpha^2\mathcal{S}_{qc}^\phi\Theta^2/[2(2\pi)^2]$	$\alpha^2\mathcal{S}_{qk}^\phi\Theta/[2(2\pi)^2]$	$\alpha^2\mathcal{S}_{kk}^\phi/(2\pi)^2$
Γ_a^ϕ	$6\psi^{-1/3}\tilde{\Gamma}_{qc}^\phi$	$6\psi^{-2/3}\tilde{\Gamma}_{qk}^\phi$	$2\tilde{\Gamma}_{kk}^\phi$
$E_{\rm min}^{\phi,a}$	$\psi m_\phi c^2\sqrt{m_\phi cL/\hbar}$	$\psi m_\phi c^2\sqrt{m_\phi cL/\hbar}$	$m_\phi c^2$
$E_{\rm max}^{\phi,a}$	$[(\mu^2L^2)(\mu\hbar c)]^{1/4}$	$(\mu\hbar c)^{1/2}$	$(\mu\hbar c)^{1/2}$

$$\frac{dN^{\rm Yu}}{dE} = \frac{1}{E_\phi}, \quad (26)$$

with $m_\nu \ll E \le E_\phi$.

Therefore, the total number of neutrinos emitted from a cosmic string loop is also independent of the neutrino energy,

$$\frac{dN_a^{\rm Yu}}{dE} = \tilde{\Gamma}_a^{\rm Yu}\left(\frac{\lambda_\phi}{L}\right)^{q_a^{\rm Yu}}\frac{\mu\lambda_\phi^2}{\hbar c}\frac{1}{m_\phi c^2}, \quad (27)$$

with all variable definitions in Table IV.

2. Cascade

After the heavy scalar decays, a cascade of particles decays ensues, of which neutrinos are one of the end products. In accordance with previous studies [36–39], we assume that the decay spectra follows a power law with index ~ -2 and that approximately all of the energy is transferred to pions, which then decay to give half of their energy to neutrinos. After imposing conservation of energy in the decay between neutrinos and the heavy real scalar we obtain

$$\frac{dN^{\rm casc}}{dE} = \frac{b_*}{2}\frac{E_\phi}{E^2}, \quad (28)$$

with $b_* = \log(E_{\rm max}^{\rm casc}/E_{\rm min}^{\rm casc})^{-1}$. As a result, the total number of neutrinos emitted from a cosmic string loop is

TABLE IV. Yukawa variable definitions.

a	Quasicusp	Quasikink	Kink-kink
$q_a^{\rm Yu}$	1/2	0	0
$\tilde{\Gamma}_a^{\rm Yu}$	$(3/7)\psi^{-7/3}\tilde{\Gamma}_{qc}^\phi$	$(3/8)\psi^{-8/3}\tilde{\Gamma}_{qk}^\phi$	$(1/3)\tilde{\Gamma}_{kk}^\phi$
$E_{\rm min}^{\rm Yu,a}$	$m_\nu c^2$	$m_\nu c^2$	$m_\nu c^2$
$E_{\rm max}^{\rm Yu,a}$	$E_{\rm max}^{\phi,qc}$	$E_{\rm max}^{\phi,qk}$	$E_{\rm max}^{\phi,kk}$

TABLE V. Cascade variable definitions, with $Q_h = 1$ GeV the hadronization energy scale.

a	Quasicusp	Quasikink	Kink-kink
$q_a^{\rm casc}$	$-1/2$	0	0
$\Gamma_a^{\rm casc}$	$(1/4)\Gamma_{qc}^{\phi}$	$(1/4)\Gamma_{qk}^{\phi}$	$(1/4)\Gamma_{kk}^{\phi}$
$E_{\rm min}^{\rm casc,a}$	$(1/2)\sqrt{m_\phi c^2 Q_h}$	$(1/2)\sqrt{m_\phi c^2 Q_h}$	$(1/2)\sqrt{m_\phi c^2 Q_h}$
$E_{\rm max}^{\rm casc,a}$	$0.1E_{\rm max}^{\phi,qc}$	$0.1E_{\rm max}^{\phi,qk}$	$0.1E_{\rm max}^{\phi,kk}$

$$\frac{dN_a^{\rm casc}}{dE} = \tilde{\Gamma}_a^{\rm casc} b_* \left(\frac{\lambda_\phi}{L}\right)^{q_a^{\rm casc}} \frac{\mu\lambda_\phi}{E^2}, \tag{29}$$

with all variable definitions in Table V.

V. STRING LOOP POPULATION

A loop of initial length L_i at time t_i will contract as it radiates energy from various string features. For the string interaction models presented here, this energy may either be in the form of gravitational waves, neutrinos, or real scalar fields. However, we do not consider emission via all these channels at once. Instead, in order to determine the evolution of the loop distribution function, we consider emission in a pair of channels: first, from gravitational waves and second, from a single specified particle model. This choice is done because cosmic string loops are always expected to radiate gravitationally, and our models are an addition beyond the standard framework. As a result, the center of mass energy μL of a loop decreases over time according to

$$\mu\frac{dL}{dt} = -\Gamma_g G\mu^2 c^{-3} - P_a^e, \tag{30}$$

with $\Gamma_g \in [50, 100]$. The first term encodes loop emission of gravitational waves, while the second term specifies the emission e from string feature a. Moreover, loops with length $L > L_a^e = \ell_e[(\Gamma_a^e/\Gamma_g)/(G\mu c^{-4})]^{1/p_a^e}$ emit more energy in the form of gravitational waves than from emission e from string feature a.

In general, Eq. (30) does not have an analytic solution for arbitrary initial loop length. However, loops with $L_i < L_a^e$ will always emit more particles than gravitational waves, and those with $L_i \gg L_a^e$ more gravitational waves than particles. Therefore we solve for the evolution of loop length with these two conditions. Moreover, in practice, the condition $L_i \gg L_a^e$ is relaxed to $L_i > L_a^e$, so that there are only two regimes:

$$L(t_i, t, L_i) = [L_i^{1+p_a^e} - (L_{\rm min}^{e,a})^{1+p_a^e}]^{\frac{1}{1+p_a^e}}\Theta(L_a^e - L_i) + [L_i - \Gamma_g G\mu c^{-3}(t - t_i)]\Theta(L_i - L_a^e), \tag{31}$$

which can be piecewise inverted to solve for L_i as a function of L. Here, $L_{\rm min}^{e,a} = [(1 + p_a^e)\Gamma_a^e c(t - t_i)\ell_e^{p_a^e}]^{1/(1+p_a^e)}$.

While some cosmic string loops are present at the initial $U(1)$ phase transition, most are formed after string segments intersect and commute, breaking off into smaller loops. Here, we assume this string loop population has relaxed to a steady-state self-similar solution. As a result, we neglect terms that involve string collision and string self-interactions. While these loops are produced both during periods of radiation and matter domination, those produced during matter domination are less abundant [40]. Therefore, we write the loop distribution as $dn^{\rm loop}/dL = dn_r^{\rm loop}/dL$, with

$$\frac{dn_r^{\rm loop}(t, L)}{dL} = \frac{\zeta_r}{2}\frac{a_{\rm eq}^3}{[a(t_{\rm eq})\chi(t_{\rm eq})]^{3/2}L_0^{5/2}}\left(\frac{L}{L_0}\right)^p \times \begin{cases} \Theta(\beta_r - \frac{L}{2ct}) & t \le t_{\rm eq} \\ \Theta(\beta_r - \frac{L_{eq}}{2ct_{\rm eq}}) & t > t_{\rm eq} \end{cases} \tag{32}$$

the distribution of loops created during radiation-domination at a time t [41]. Moreover, $t_{\rm eq}$ is the time of matter-radiation equality, χ the comoving horizon distance, $\zeta_r = 1.04$ a normalization factor, $\beta_r = 0.05$ the typical scale of loops produced radiation domination relative to the size of the horizon. Finally, $L_0 = L_i(0, t, L)$ and $L_{\rm eq} = L_i(t_{\rm eq}, t, L)$ are the lengths of a loop at $t = 0$ and $t_{\rm eq}$. We show some example distributions for cosmic string loops in Figs. 3 and 4.

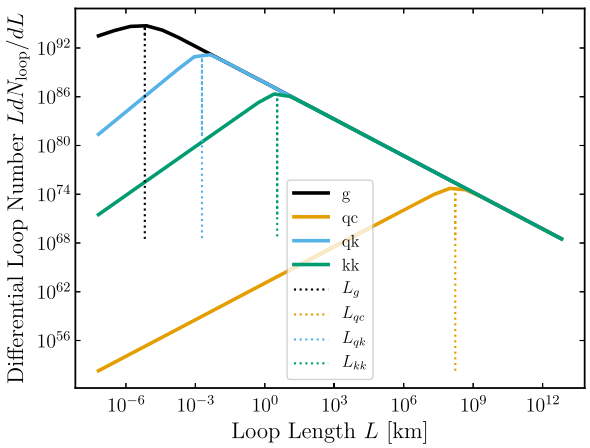

FIG. 3. The differential loop number $dN_{\rm loop}/dL = \chi^3 dn_{\rm loop}/dL$, with χ the size of the comoving horizon, evaluated at $z = 0$. The solid black line is the number assuming only gravitational emission, while the solid orange (blue) [green] line is due to both gravitational emission and AB emission from quasicusps (quasikinks) [kink-kink collisions]. The vertical dotted lines indicate the length $L_{\rm min}^{e,a}$.

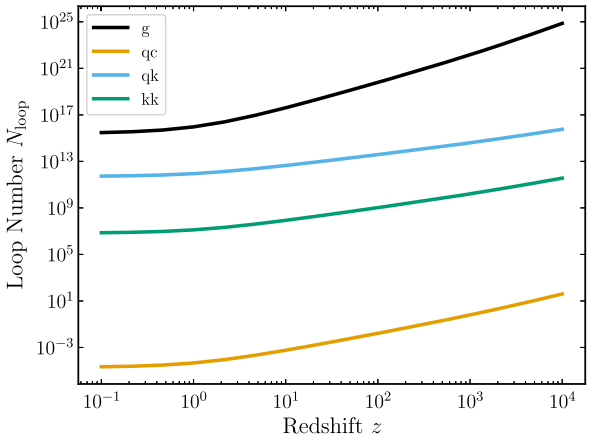

FIG. 4. The number of loops $N_{\rm loop} = \chi^3 n_{\rm loop}$, with χ the size of the comoving horizon, as a function of redshift. The label and color scheme follow that of Fig. 3. Hence, loop distributions with smaller $L_{\rm min}$ have higher numbers.

VI. RESULTS

Given the emission spectra of neutrinos from a single cosmic string loop, as well as the distribution of cosmic string loops, we now present both the source function and flux for each phenomenological case. We then use the dominant flux to place an upper bound on the fraction f_a^e of HEAN sourced by cosmic string loops. The bounds are obtained in the following manner.

First, evaluating Eq. (2), we obtain

$$S_a^e(t,E) = cA_a^e \frac{dN_a^e[E, L_{\rm min}^{e,a}(t)]}{dE} \frac{dn_{\rm loop}[0, L_{\rm min}^{e,a}(t)]}{dL}, \tag{33}$$

$$A_a^e \equiv \frac{4}{1+p_a^e} \frac{\Gamma(\frac{5+2q_a^e}{2+2p_a^e})}{\Gamma(\frac{7+2p_a^e+2q_a^e}{2+2p_a^e})} \times {}_2F_1\left[1+\frac{3}{2+2p_a^e}, \frac{5+2q_a^e}{2+2p_a^e}, \frac{7+2p_a^e+2q_a^e}{2+2p_a^e}, -1\right], \tag{34}$$

with $\Gamma(n)$ the gamma function, and ${}_2F_1(a,b,c,d)$ a hypergeometric function. In this expression, we recall that $a \in \{qc, qk, kk\}$ and $e \in \{(2), \mathrm{AB}, \mathrm{Yu}, \mathrm{casc}\}$.

We define the index of the local energy spectrum through the expression $dN_a^e/dE \propto E^{-\gamma_a^e}$. Using Eqs. (4) and (33), we evaluate Eq. (1), after changing variables from time to redshift via $dt/dz = -1/[H(z)(1+z)]$, to obtain

$$\Phi_a^e(t,E) = I_a^e(t,E) \frac{c^2}{H_0} \frac{dN_a^e[E, L_{\rm min}^{e,a}(t)]}{dE} \frac{dn_{\rm loop}[0, L_{\rm min}^{e,a}(t)]}{dL} \tag{35}$$

$$I_a^e(t,E) \equiv A_a^e \int_{z(t)}^{z_\nu(t,E)} \frac{dz}{E(z)} (1+z)^{-\gamma_a^e} f(z)^{-(q_a^e+\frac{5}{2})/(p_a^e+1)}, \tag{36}$$

TABLE VI. Tabulated values for $I_a^e(t_0, E_{\rm min})$, $E_{\rm min} = 16$ TeV, with a specified by the column and e by the row. For emission of type (2), quasicusps and quasikinks are helicity suppressed, and so we do not consider them here.

I_a^e	Quasicusp	Quasikink	Kink-kink
(2)	N/A	N/A	4.35×10^{10}
AB	94900	15.2	241
Yu	3.25×10^{11}	2.40×10^{6}	2.40×10^{6}
casc	2.56	2.04	2.04

with $H(z) = H_0 E(z)$ the Hubble parameter, H_0 Hubble's constant, $E(z) = [\Omega_m(1+z)^3 + (1-\Omega_m) + \Omega_r(1+z)^4]^{1/2}$ for Λ cold dark matter (ΛCDM), Ω_m the matter-density parameter, Ω_r the radiation-density parameter, and $f(z) = t(z)/t$. We present the values for $I_a^e(t_0, E_{\rm min})$ in Table VI using Planck 2018 parameters [42].

As indicated by Fig. 5 all spectra follow a power law with a sharp cutoff. As a result, to make an easy connection with observation, we reparametrize the neutrino spectrum $\Phi_a^e(t_0, E)$ today as the following two-parameter model,

$$\Phi_a^e(t_0,E) \simeq C_0 B_a^e (E/E_0)^{-\beta_a^e} \Theta(E - E_{\rm max}^{e,a}) \Theta(E - E_{\rm min}^{e,a}), \tag{37}$$

with $C_0 = 2 \times 10^{-18}\,\mathrm{GeV}^{-1}\,\mathrm{cm}^{-2}\,\mathrm{s}^{-1}\,\mathrm{sr}^{-1}$ and $E_0 = 100\,\mathrm{TeV}$. Note that, for most cosmic string parameter values, $E_{\rm min}^{a,e}$ is much smaller than observed HEAN energies, and so the low-energy cutoff can be ignored. We write this equation as an approximate equality as the spectral index β_a^e has a nonzero running with energy, $d\beta_a^e/dE \neq 0$. However, this running is small, and so we average its value over the

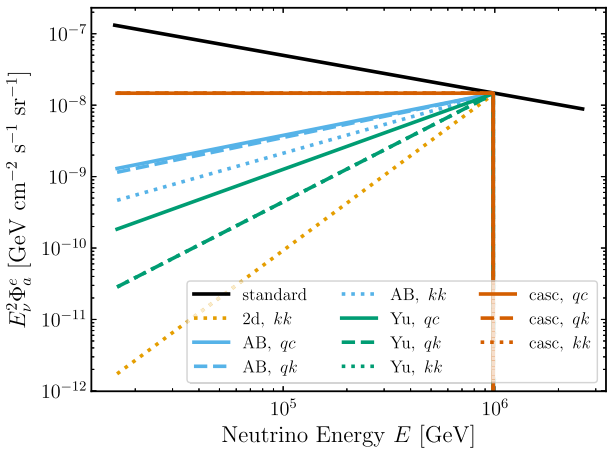

FIG. 5. Spectra of HEAN emitted from cosmic strings using Eq. (37) compared with the observed HEAN spectrum (in solid black) using Eq. (39). The orange (blue) [green] {red} line indicates HEAN emission via the (2) (AB) [Yu] {casc} model. Moreover, solid (dashed) [dotted] lines indicate that the string population contains quasicusps (quasikinks) [kink-kink collisions]. We choose $E_{\rm max}^{e,a} = 10^6$ GeV. For large enough amplitude values, the spectrum may appear as a bump before the sharp cutoff.

TABLE VII. Tabulated values for β_a^e, with a specified by the column and e by the row.

β_a^e	Quasicusp	Quasikink	Kink-kink
(2)	N/A	N/A	−0.27
AB	1.37	1.38	1.14
Yu	0.855	0.439	0.439
casc	2	2	2

observed energy range. Moreover, note that $\beta_a^e \neq \gamma_a^e$ as the energy dependence of the neutrino horizon shifts the spectral index, which we show in Table VII. We show the dependence of the amplitude B_a^e on our model parameters in Table VIII. In order to save space in the table, we include a scaling of the b_* parameter in Eq. (38). Using the new parametrization of Eq. (37), we plot some example spectra in Fig. 5:

$$\exp(b_*) = 1640\left(\frac{G\mu c^{-4}}{4.5\times10^{-24}}\right)^{1/2}\left(\frac{m_\phi c^2}{10^7\ \mathrm{GeV}}\right)^{1/2}. \quad (38)$$

We now identify the viable parameter space of cosmic string HEAN emission subject to the constraint that it is not greater than the observed HEAN spectrum, $\Phi_a^e(E) \leq \Phi_{\mathrm{HEAN}}(E)$, for all energies. We model the observed HEAN spectrum as a power law with spectral index $\gamma = 2.28$ [1],

$$\Phi_{\mathrm{HEAN}}(E) = C_0\Phi_0(E/E_0)^{-\gamma}, \quad (39)$$

with $\Phi_0 = 1.66$. We take the observed HEAN energy range to be $E_{\mathrm{min}} = 16\ \mathrm{TeV} \leq E \leq E_{\mathrm{max}} = 2.6\ \mathrm{PeV}$. As a result, the three equations

$$B_a^e \leq \Phi_0(E_{\mathrm{max}}^{e,a}/E_0)^{\beta_a^e-\gamma}, \quad (40)$$

$$E_{\mathrm{min}} \leq E_{\mathrm{max}}^{e,a} \leq E_{\mathrm{max}}, \quad (41)$$

$$E_{\mathrm{min}}^{e,a} \leq E_{\mathrm{max}}^{e,a} \quad (42)$$

define a region in the cosmic-string parameter space that is viable to contribute to the HEAN flux and whose upper bound we show in Fig. 6. Parameters that are above this upper bound are ruled out, as they would lead to a HEAN spectrum larger than what we observe. In order to relate these equations to the original parameters, one can use the formulas listed in Tables VII and VIII, along with the definition of $E_{\mathrm{max}}^{e,a}$ listed in the Tables in Sec. IV.

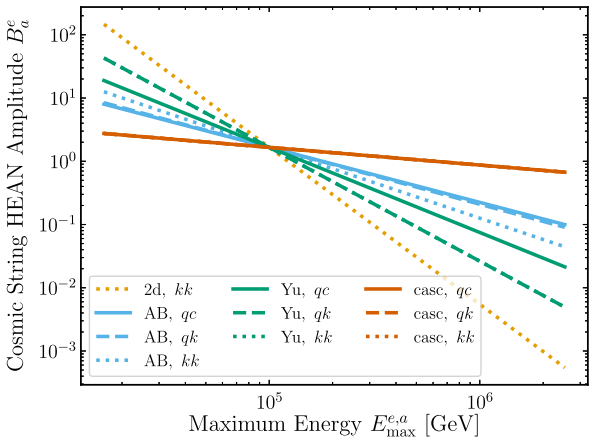

FIG. 6. The maximum amplitude B_a^e of HEANs that come from a population of cosmic-string loops using Eq. (40). The orange (blue) [green] {red} line indicates HEAN emission via the (2) (AB) [Yu] {casc} model. Moreover, solid (dashed) [dotted] lines indicate that the string population contains quasicusps (quasikinks) [kink-kink collisions]. All lines intersect at $E_{\mathrm{max}}^{e,a} = E_0$ by construction of our parametrization. Values of B_a^e above a given line are ruled out. Table VIII translates these amplitudes into cosmic-string parameters.

We note that, for the chosen loop distribution model of Ref. [41], the strongest constraints on the string tension come from pulsar timing arrays, which set the limit $G\mu c^{-4} \lesssim 10^{-10}$ [43,44]. Hence, in Table VIII, we always choose smaller fiducial tension values that are not ruled out by such observations. We find that, for the largest possible string tensions, direct kink-kink couplings require amplitudes $\tilde{\Gamma}_{kk}^{(2)} \sim 10^{13}$ to make a sizeable fraction of the observed HEAN spectrum. These values are much larger than expected from Table I. That is, such amplitudes require $\mathcal{S}_{\mathrm{kk}} \sim 500$ and a population of strings with a large number of features [i.e., $\mathcal{O}(10^{11})$ kinks]. Therefore, we expect such

TABLE VIII. Tabulated values for B_a^e, with a specified by the column and e by the row. The scaling of b_* is shown in Eq. (38). Fiducial values are chosen so that they are not ruled out by HEAN spectra observations.

B_a^e	Quasicusp	Quasikink	Kink-kink
(2)	N/A	N/A	$1.09\times10^{-4}\left(\frac{\tilde{\Gamma}_{kk}^{(2)}}{3.16\times10^{13}}\right)^{-1/4}\left(\frac{G\mu c^{-4}}{4.5\times10^{-11}}\right)^{-3/8}$
AB	$0.383\left(\frac{\tilde{\Gamma}_{qc}^{\mathrm{AB}}}{10^{-25}}\right)^{-2/3}\left(\frac{G\mu c^{-4}}{4.5\times10^{-26}}\right)^{5/12}$	$2.71(\tilde{\Gamma}_{qk}^{\mathrm{AB}})^{-3/14}\left(\frac{G\mu c^{-4}}{1.2\times10^{-27}}\right)^{17/21}$	$0.0212(\tilde{\Gamma}_{kk}^{\mathrm{AB}})^{-1/4}\left(\frac{G\mu c^{-4}}{4.5\times10^{-30}}\right)^{5/8}$
Yu	$0.569\left(\frac{\tilde{\Gamma}_{qc}^{\mathrm{Yu}}}{10^{-28}}\right)^{-1}\left(\frac{G\mu c^{-4}}{4.5\times10^{-26}}\right)\left(\frac{m_\phi c^2}{10^5\ \mathrm{GeV}}\right)^{-5/2}$	$9.28(\tilde{\Gamma}_{qk}^{\mathrm{Yu}})^{-1/4}\left(\frac{G\mu c^{-4}}{1.4\times10^{-28}}\right)\left(\frac{m_\phi c^2}{10^5\ \mathrm{GeV}}\right)^{-7/4}$	$62.8(\Gamma_{kk}^{\mathrm{Yu}})^{-1/4}\left(\frac{G\mu c^{-4}}{4.5\times10^{-31}}\right)\left(\frac{m_\phi c^2}{10^5\ \mathrm{GeV}}\right)^{-7/4}$
casc	$\frac{3.42}{1000}\left(\frac{b_*}{7.4}\right)\left(\tilde{\Gamma}_{qc}^{\mathrm{casc}}\right)^{-1/3}\left(\frac{G\mu c^{-4}}{4.5\times10^{-24}}\right)\left(\frac{m_\phi c^2}{10^7\ \mathrm{GeV}}\right)^{1/6}$	$28.2\left(\frac{b_*}{7.4}\right)\left(\tilde{\Gamma}_{qk}^{\mathrm{casc}}\right)^{-1/4}\left(\frac{G\mu c^{-4}}{4.6\times10^{-24}}\right)\left(\frac{m_\phi c^2}{10^7\ \mathrm{GeV}}\right)^{1/4}$	$307\left(\frac{b_*}{7.4}\right)\left(\tilde{\Gamma}_{kk}^{\mathrm{casc}}\right)^{-1/4}\left(\frac{G\mu c^{-4}}{4.5\times10^{-24}}\right)\left(\frac{m_\phi c^2}{10^7\ \mathrm{GeV}}\right)^{1/4}$

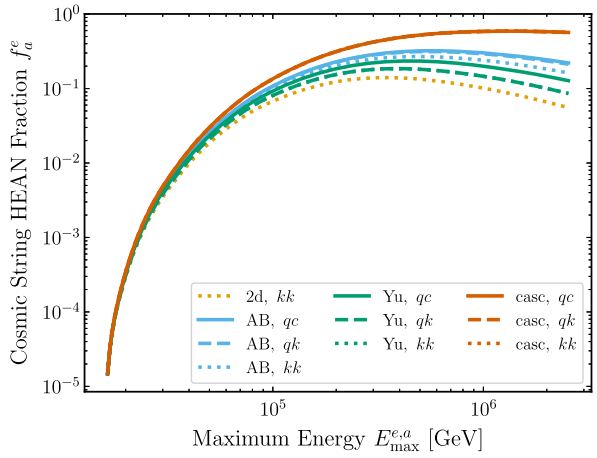

FIG. 7. The maximum fraction of HEANs that come from a population of cosmic-string loops using Eq. (43) with Eqs. (37) and (39). The orange (blue) [green] {red} line indicates HEAN emission via the (2) (AB) [Yu] {casc} model. Moreover, solid (dashed) [dotted] lines indicate that the string population contains quasicusps (quasikinks) [kink-kink collisions].

direct couplings cannot give rise to a sizeable fraction of observed HEANs. All other cases are still viable.

More precisely, the fraction f_a^e of observed neutrinos associated with a cosmic-string spectrum given by emission model e and string feature a is then

$$f_a^e = \frac{\int_{E_{\min}}^{E_{\max}} dE A_{\rm eff}(E)\Phi_a^e(t_0,E)}{\int_{E_{\min}}^{E_{\max}} dE A_{\rm eff}(E)\Phi_{\rm HEAN}(E)}, \tag{43}$$

with $A_{\rm eff}(E)$ the effective area of IceCube for muon neutrinos, which we take from Ref. [45]. We plot the maximum contribution of cosmic string loops [i.e., when $\Phi_a^e(t_0, E_{\max}^{e,a}) = \Phi_{\rm HEAN}(E_{\max}^{e,a})$] in Fig. 7 and find that with the parameters chosen, $f_a^e \lesssim 59\%$.

VII. DISCUSSION

We clarify five assumptions and present seven comments. First, in each model of neutrino emission we assume a single neutrino. If there are multiple neutrino species coupled to the string, then energy extracted from the loop will be a sum over all neutrino emission channels. Moreover, since cosmic strings are distant objects, then the observed spectrum of neutrinos will be a sum of the spectrum of each neutrino channel weighed by the corresponding probability of oscillating into that neutrino. Note that even if there is only one neutrino coupled, then flavor oscillations will decrease the spectral amplitude in that flavor. Regardless, the effects of oscillations can always be absorbed into a redefinition of $\tilde{\Gamma}$, and so our results can be scaled appropriately to include them.

Second, if the neutrino is a Majorana fermion instead of a Dirac fermion, then $\bar{\nu} = \nu^{\rm T}\mathcal{C}$ with $\mathcal{C}$ the charge conjugation matrix. This replacement will not change the spectral index, and should not change the amplitude of emission by more than an $\mathcal{O}(1)$ coefficient.

Third, for the indirect emission models, we assume the heavy real scalar instantaneously decays into neutrinos.

Fourth, we did not consider cosmic-string loop populations with multiple features (e.g., loops that have both quasikinks and quasicusps). Current simulations, without considering backreaction effects, estimate that ∼40% of the string loops contain cusps and $\mathcal{O}(1)$ have on average four kinks [46]. Since cusps extract more energy from the string than kinks and quasikinks, but typically have smaller amplitudes, we expect that the presence of cusps would decrease the expected amplitude in the HEAN energy range (or alternatively, the presence of kinks to increase the amplitude). Thus, our results safely represent an upper limit on the possible contribution of cosmic strings to the HEAN spectrum.

Fifth, we assume that the population of cosmic string is characterized by a single string tension value. Instead, it is possible that there exist multiple varieties of cosmic strings in the Universe, with each cosmic string characterized by a different string tension, and thus the resulting spectrum would be the sum of these two types of strings. In addition, the string tension may have some time dependence [47], leading to a HEAN spectrum that would be average over the distribution of tension values. Both of these cases are beyond the scope of this work.

While we do consider a wide variety of emission models here, the list is not exhaustive. For example, we did not consider two-body emission of real scalars from cosmic strings that then decay in HEAN. In the case of two-body emission of real scalars, this model would not change the spectrum index of emission relative to its one-body counterpart. This similarity is because the index is controlled by the Yukawa and cascade decays. Therefore, while the precise values for the amplitude $\tilde{\Gamma}$ may change, the maximum contribution to the HEAN spectrum will not.

In addition to emission models, it is also possible that cosmic strings collide and annihilate with one another into neutrinos. However, cosmic strings are very thin, and so their annihilation cross section is very small. Thus, we do not expect such a process to contribute greatly.

Even though we find that the models presented are a subdominant portion of the total spectrum, the presence of a sharp cutoff implies that HEANs from cosmic strings may present as a distinct bump in the observed HEAN spectrum, opening up the possibility for their detection. Moreover, if cosmic strings exist, their gravitational wells would alter energies of traversing photons. Hence, in principle, cross correlations of HEAN maps with the cosmic microwave background would be able to distinguish cosmic strings from other subdominant contributions, although we expect such a signal to be very small.

In each of our plots in Sec. VI, the region to the right of the orange dashed line requires either values of the

coupling constant or string feature parameters that are greater than $\mathcal{O}(1)$. It is both difficult to create such a theory and at odds with the perturbative approach we took to calculate the spectra. Despite this, we leave this region in our plots as it may be the case other models with similar effective parameters and spectral indices are viable.

Moreover, in these plots, we only consider the constraints on the effective parameters describing HEAN emission from cosmic strings. At higher neutrino energies, where current and future experiments like ANITA [48] and POEMMA [49] can observe neutrinos, there will be additional constraints. The future upgrade of IceCube-Gen2 [20] will also allow detections of HEANs at lower energies, thus extending the range of our plots. In addition, in the cascade case, there will be an emission of gamma rays that go along with the neutrinos. Treatment of both of these effects are a work in progress and beyond the scope of this work.

While Fig. 7 shows that cosmic strings can contribute no more than 59% of the entire HEAN flux, this result holds only if the spectral index of HEAN is precisely $\gamma = 2.28$. The uncertainty in this parameter leads to a variation in the maximum contribution. Moreover, cascade neutrino events indicate that $\gamma = 2.53$ [2]. However, for the 1σ uncertainties around a central value in either cascade or track observations, we find that the maximum contribution always lies in an $\mathcal{O}(1)$ fraction.

Finally, we note that since we took an effective field theory approach to our problem, the parameter spaces we have identified may be constrained once they are linked to a corresponding UV completion. However, it is not inconceivable that these UV completions will still have unconstrained parameter spaces for HEAN emission. Moreover, the effective models we presented also most likely have parameter constraints due to experiments and astrophysical effects. However, we suspect such constraints can be balanced by a suitable choice of amplitude string parameters. Regardless, for both cases, such an investigation is beyond the scope of this work.

VIII. CONCLUSION

In this paper we quantified the possible contribution of cosmic strings to the HEAN spectrum for a wide variety of models. First, we presented the general formula for calculating neutrino emission from distant sources and updated the calculation for the HEAN optical depth compared to previous works on cosmic-string emission. In doing so, we both employed a more accurate numerical approach and included all seven channels of Standard Model neutrino self-interactions.

Then, in order to classify possible models, we took an effective field theory approach and delineated two avenues of HEAN production: direct and indirect. In direct emission, the cosmic string emits HEANs through a direct coupling of neutrinos to the cosmic string, while in indirect emission the cosmic string emits a particle which then decays into HEANs. For both direct and indirect emission we consider two models each. That is, we considered direct emission of HEANs via a two-body emission and a Aharonov-Bohm coupling. For indirect emission, we considered the emission of a heavy real scalar which then decays into HEANs either from a Yukawa coupling or through a hadronic cascade. Aside from the cascade case, none of the other calculations have been done before.

In addition to the particular cosmic string phenomenology, the energy spectrum of HEANs is also determined by the geometry of the string. In particular, efficient cosmic-string particle emission must come either from quasicusps, quasikinks, or kink-kink collisions on the string. Previous work has not considered emission from kink-kink collisions. Therefore, for each emission model and string feature, we then calculated the local energy spectrum of HEANs emitted from the cosmic string.

Next, we calculated the distribution of cosmic-string loops that emit both gravitational waves and a given neutrino emission model that specifies a string feature. These loops are created during radiation domination and then shrink as they emit energy. We note again that the shrinking due to nongravitational emission has not been considered in previous works. In doing this calculation, we then also identified the dominant forms of energy emission in cosmic-string loops and delineated their corresponding regimes.

With the local energy spectrum and cosmic-string loop distribution specified, we then calculated the HEAN energy spectrum today using the Boltzmann equation for each emission model and string feature and obtained a simple power law with a sharp cutoff in Eq. (37), i.e., a two-parameter model. With these spectra, we then required each one must be less than the observed HEAN spectrum. This requirement led us to identify and constrain the corresponding parameter space of HEAN emission. As a result, we found that, with the models presented, cosmic strings can contribute an $\mathcal{O}(1)$ fraction of HEANs.

ACKNOWLEDGMENTS

We thank the anonymous referee for useful feedback. C. C.-S. acknowledges the support of the Bill and Melinda Gates Foundation. This work was supported at Johns Hopkins by NSF Grant No. 1818899 and the Simons Foundation. This work was finalized at the Aspen Center for Physics, which is supported by National Science Foundation Grant No. PHY-1607611.

[1] J. Stettner (IceCube Collaboration), Measurement of the diffuse astrophysical muon-neutrino spectrum with ten years of IceCube data, Proc. Sci. ICRC20192020 (**2020**) 1017 [arXiv:1908.09551].

[2] A. Schneider (IceCube Collaboration), Characterization of the astrophysical diffuse neutrino flux with IceCube high-energy starting events, Proc. Sci. ICRC2019 (**2020**) 1004 [arXiv:1907.11266].

[3] E. Waxman and J. N. Bahcall, High-Energy Neutrinos from Cosmological Gamma-Ray Burst Fireballs, Phys. Rev. Lett. **78**, 2292 (1997).

[4] R. Abbasi *et al.* (IceCube Collaboration), Search for muon neutrinos from gamma-ray bursts with the IceCube neutrino telescope, Astrophys. J. **710**, 346 (2010).

[5] R. Abbasi *et al.* (IceCube Collaboration), Limits on Neutrino Emission from Gamma-Ray Bursts with the 40 String IceCube Detector, Phys. Rev. Lett. **106**, 141101 (2011).

[6] R. Abbasi (IceCube Collaboration), An absence of neutrinos associated with cosmic-ray acceleration in γ-ray bursts, Nature (London) **484**, 351 (2012).

[7] M. G. Aartsen *et al.* (IceCube Collaboration), Search for prompt neutrino emission from gamma-ray bursts with IceCube, Astrophys. J. Lett. **805**, L5 (2015).

[8] M. G. Aartsen *et al.* (IceCube Collaboration), An all-sky search for three flavors of neutrinos from gamma-ray bursts with the IceCube neutrino observatory, Astrophys. J. **824**, 115 (2016).

[9] M. G. Aartsen *et al.* (IceCube Collaboration), Extending the search for muon neutrinos coincident with gamma-ray bursts in IceCube data, Astrophys. J. **843**, 112 (2017).

[10] F. Tavecchio, C. Righi, A. Capetti, P. Grandi, and G. Ghisellini, High-energy neutrinos from FR0 radio-galaxies?, Mon. Not. R. Astron. Soc. **475**, 5529 (2018).

[11] M. G. Aartsen *et al.* (IceCube Collaboration), The contribution of Fermi-2LAC blazars to the diffuse TeV-PeV neutrino flux, Astrophys. J. **835**, 45 (2017).

[12] D. Hooper, T. Linden, and A. Vieregg, Active galactic nuclei and the origin of IceCube's diffuse neutrino flux, J. Cosmol. Astropart. Phys. 02 (2019) 012.

[13] C. Yuan, K. Murase, and P. Mészáros, Complementarity of stacking and multiplet constraints on the blazar contribution to the cumulative high-energy neutrino intensity, Astrophys. J. **890**, 25 (2020).

[14] A. Plavin, Y. Y. Kovalev, Y. A. Kovalev, and S. Troitsky, Observational evidence for the origin of high-energy neutrinos in parsec-scale nuclei of radio-bright active galaxies, Astrophys. J. **894**, 101 (2020).

[15] A. V. Plavin, Y. Y. Kovalev, Y. A. Kovalev, and S. V. Troitsky, Directional association of TeV to PeV astrophysical neutrinos with radio blazars, Astrophys. J. **908**, 157 (2021).

[16] B. Zhou, M. Kamionkowski, and Y.-f. Liang, Search for high-energy neutrino emission from radio-bright AGN, Phys. Rev. D **103**, 123018 (2021).

[17] N. Senno, K. Murase, and P. Mészáros, Constraining high-energy neutrino emission from choked jets in stripped-envelope supernovae, J. Cosmol. Astropart. Phys. 01 (2018) 025.

[18] A. Esmaili and K. Murase, Constraining high-energy neutrinos from choked-jet supernovae with IceCube high-energy starting events, J. Cosmol. Astropart. Phys. 12 (2018) 008.

[19] M. G. Aartsen *et al.* (IceCube Collaboration), IceCube search for high-energy neutrino emission from TeV pulsar wind nebulae, Astrophys. J. **898**, 117 (2020).

[20] M. G. Aartsen *et al.* (IceCube-Gen2 Collaboration), IceCube-Gen2: The window to the extreme Universe, J. Phys. G **48**, 060501 (2021).

[21] V. Berezinsky, E. Sabancilar, and A. Vilenkin, Extremely high energy neutrinos from cosmic strings, Phys. Rev. D **84**, 085006 (2011).

[22] C. Lunardini and E. Sabancilar, Cosmic strings as emitters of extremely high energy neutrinos, Phys. Rev. D **86**, 085008 (2012).

[23] J. M. Hyde, A. J. Long, and T. Vachaspati, Dark strings and their couplings to the Standard Model, Phys. Rev. D **89**, 065031 (2014).

[24] A. J. Long, J. M. Hyde, and T. Vachaspati, Cosmic strings in hidden sectors: 1. Radiation of standard model particles, J. Cosmol. Astropart. Phys. 09 (**2014**) 030.

[25] A. J. Long and T. Vachaspati, Cosmic strings in hidden sectors: 2. Cosmological and astrophysical signatures, J. Cosmol. Astropart. Phys. 12 (**2014**) 040.

[26] T. Vachaspati and A. Vilenkin, Gravitational radiation from cosmic strings, Phys. Rev. D **31**, 3052 (1985).

[27] M. Hindmarsh, Gravitational radiation from kinky infinite strings, Phys. Lett. B **251**, 28 (1990).

[28] B. Allen and E. P. S. Shellard, Gravitational radiation from cosmic strings, Phys. Rev. D **45**, 1898 (1992).

[29] T. Vachaspati, Cosmic rays from cosmic strings with condensates, Phys. Rev. D **81**, 043531 (2010).

[30] T. Damour and A. Vilenkin, Gravitational wave bursts from cusps and kinks on cosmic strings, Phys. Rev. D **64**, 064008 (2001).

[31] P. Auclair, D. A. Steer, and T. Vachaspati, Particle emission and gravitational radiation from cosmic strings: Observational constraints, Phys. Rev. D **101**, 083511 (2020).

[32] C. Creque-Sarbinowski, J. Hyde, and M. Kamionkowski, Resonant neutrino self-interactions, Phys. Rev. D **103**, 023527 (2021).

[33] Y. Ema, R. Jinno, and T. Moroi, Cosmic-ray neutrinos from the decay of long-lived particle and the recent IceCube result, Phys. Lett. B **733**, 120 (2014).

[34] K. Jones-Smith, H. Mathur, and T. Vachaspati, Aharonov-Bohm radiation, Phys. Rev. D **81**, 043503 (2010).

[35] M. G. Alford and F. Wilczek, Aharonov-Bohm Interaction of Cosmic Strings with Matter, Phys. Rev. Lett. **62**, 1071 (1989).

[36] V. Berezinsky and M. Kachelriess, Monte Carlo simulation for jet fragmentation in SUSY QCD, Phys. Rev. D **63**, 034007 (2001).

[37] S. Sarkar and R. Toldra, The High-energy cosmic ray spectrum from relic particle decay, Nucl. Phys. **B621**, 495 (2002).

[38] C. Barbot and M. Drees, Detailed analysis of the decay spectrum of a super heavy X particle, Astropart. Phys. **20**, 5 (2003).

[39] R. Aloisio, V. Berezinsky, and M. Kachelriess, Fragmentation functions in SUSY QCD and UHECR spectra produced in top—down models, Phys. Rev. D **69**, 094023 (2004).

[40] E. J. Copeland, T. W. B. Kibble, and D. A. Steer, The evolution of a network of cosmic string loops, Phys. Rev. D **58**, 043508 (1998).
[41] J. J. Blanco-Pillado, K. D. Olum, and B. Shlaer, The number of cosmic string loops, Phys. Rev. D **89**, 023512 (2014).
[42] N. Aghanim *et al.* (Planck Collaboration), Planck 2018 results. VI. Cosmological parameters, Astron. Astrophys. **641**, A6 (2020); **652**, C4(E) (2021).
[43] P. D. Lasky *et al.*, Gravitational-Wave Cosmology Across 29 Decades in Frequency, Phys. Rev. X **6**, 011035 (2016).
[44] R. Abbott *et al.* (LIGO Scientific, Virgo, and KAGRA Collaborations), Constraints on Cosmic Strings Using Data from the Third Advanced LIGO–Virgo Observing Run, Phys. Rev. Lett. **126**, 241102 (2021).
[45] M. G. Aartsen (IceCube Collaboration), Evidence for high-energy extraterrestrial neutrinos at the IceCube detector, Science **342**, 1242856 (2013).
[46] C. J. Copi and T. Vachaspati, Shape of cosmic string loops, Phys. Rev. D **83**, 023529 (2011).
[47] M. Yamaguchi, Cosmological evolution of cosmic strings with time dependent tension, Phys. Rev. D **72**, 043533 (2005).
[48] A. V. Olinto *et al.* (POEMMA Collaboration), The POEMMA (Probe of Extreme Multi-Messenger Astrophysics) observatory, J. Cosmol. Astropart. Phys. 06 (2021) 007.
[49] P. W. Gorham *et al.* (ANITA Collaboration), Constraints on the ultrahigh-energy cosmic neutrino flux from the fourth flight of ANITA, Phys. Rev. D **99**, 122001 (2019).